Chimica Techno Acta
published by Ural Federal University
eISSN 2411-1414
chimicatechnoacta.ru

ARTICLE
2024, vol. 11(1), No. 202411107
DOI: 10.15826/chimtech.2024.11.1.07

# Modification of bacterial cellulose using silk fibroin β-sheet crystals induced by ultrasonication

Mary Stephanie Carranza [ab *], Neil Andrew D. Bascos [a], Maria Carmen Tan [b], Francisco Franco Jr. [b]

**a:** Protein, Proteomics and Metabolomics Facility, University of the Philippines System – Philippine Genome Center, Quezon City 1101, Philippines
**b:** Chemistry Department, De La Salle University, Manila 0922, Philippines
***** Corresponding author: mscarranza@up.edu.ph

This paper belongs to a Regular Issue.

## Abstract

Silk fibroin (SF) has been continuously explored as a biomaterial due to its biocompatibility, tunability, and self-healing properties. In this work, we present a novel approach to the modification of bacterial cellulose (BC) with SF β-sheet dominant structures induced via ultrasonication. Secondary structure analysis through infrared spectroscopy, thioflavin T assay, and circular dichroism spectropolarimetry revealed a conversion of silk I to silk II structures within the protein mixture. Cold field emission scanning electron microscope images revealed the tightly packed fibers coated with the protein. Thermogravimetric curves demonstrated higher resistance to temperature degradation supplemented by broader and flatter DSC curves attributed to the highly bonded and dense composite. Successful conversion of amide I to amide II and amide III allowed for the more stable β-crystals to contribute to a more thermodynamically stable double-network hydrogel. The conversion of silk I to silk II structures offers a viable and highly biocompatible material that is both thermodynamically and biochemically stable for various potential biomedical applications.

## Keywords

silk fibroin
β-sheet crystals
bacterial cellulose
composite

**Received**: 11.01.24
**Revised**: 30.01.24
**Accepted**: 30.01.24
**Available online**: 05.02.24

## Key findings

- Ultrasonication of regenerated SF absorbed by BC hydrogels allowed for entrapment of a mixture of silk I- and silk II-dominant structured proteins.
- Beta-sheet crystals formed allowed for a more thermodynamically stable double-network hydrogel.
- Ultrasonication of BC-SF composites is a facile and novel method for developing biomaterial applications.



## 1. Introduction

As a highly versatile and functional biomaterial, silk fibroin has been a material of large interest due to its high biocompatibility, low immunogenicity, and tunability. These properties are highly preferred in specific fields, including the medical device industry, where characteristics such as mechanical resistance, temperature degradability, permeability, and tensile strength, must be considered to accommodate both the mechanical and biological functions of a biomaterial [1]. Silk, which is a component of various economically noteworthy products with remarkable mechanical properties has been utilized for thousands of years. Bombyx mori silkworms are domestic insects used internationally as a source of fabric [2–4]. The popularity of this biomaterial has been attributed to its exceptional mechanical properties, biocompatibility with a diversity of cell types, the potential for proteolytic breakdown, and the minimal inflammatory property of SF [5, 6]. The only drawback is that solvents with high ionic strength are needed to disrupt the resilient hydrogen bonds, strengthening the β-sheet molecular silk assembly. Upon removal of the high salt concentration, usually by dialysis, the ionic force decreases, causing the SF solution to be in a sol-gel transition which is metastable. As demonstrated in the paper by Matsumoto, the morphology of SF was found to be dependent on the protein concentration, temperature, and pH during gelation [7]. Since SF chains were found to possess a tendency to

aggregate, it was reported that the displayed amorphous or random coiling could transform into a more stable β-sheet conformation. These β-sheet structures have been known to stabilize the hydrogel and require more rigorous means to degrade either through enzymatic or oxidative procedures [7–9].

Another unique biomaterial, bacterial cellulose (BC), is produced by single-cell acetic acid-producing bacterial strains within the genus Acetobacter, Gluconobacter, Gluconacetobacter, and Komagateibacter. Some species of the genus Gluconacetobacter and Komagateibacter were reported to generate a hydrated extracellular matrix of crystalline cellulose [10–12]. These distinctive nanofibers were extruded from BC, exhibiting elevated water absorptivity and gaseous permeability [13, 14]. For this reason, the BC-fashioned products allowed for the exchange of nutrients and other entities needed to sustain the life of the bacteria [15]. The BC hydrogels were found to be inherently pure and did not necessitate a purification process. BC nanofibers exhibited nanofibers that were thinner by 100 times than conventional plant-based cellulose. BC manifested a substantially porous 3D structure that could be biocompatible with other materials [16, 17].

Various researchers have investigated a range of techniques to enhance disparate characteristics to produce intricate scaffolds for biomedical applications [18, 19]. In one instance, authors prepared BC/SF nanoribbon composites and observed the improvement of the mechanical properties of SF [20]. However, the method used compromised the crystallinity of BC as the nanocellulose was homogenized prior to blending with SF. Another research group utilized a technique where soaking time of BC composites in regenerated silk fibroin led to the synthesis of BC-SF cube-like hydrogels [21]. This study was unable to exploit the amyloidogenic nature of silk fibroin which can be useful for 'entrapping' proteins/molecules in place within the fine BC fibers. In this paper, we report a novel method where ultrasonication was used to lock silk fibroin in producing a BC-SF composite. The resulting composite was further characterized for structural changes.

## 2. Materials and Methods

### 2.1. Reagents and materials

Raw silk was obtained from the OISCA-Bago Training Center at Negros Occidental. Chemicals used for the silk fibroin (SF) extraction included sodium carbonate ($Na_2CO_3$, Duksan), sodium bicarbonate ($NaHCO_3$, Sigma Aldrich), calcium chloride ($CaCl_2$, Sigma-Aldrich), and absolute ethanol ($CH_3CH_2OH$, Scharlau). Dialysis membranes (10K MWCO, SciLab) were used for the purification step. Commercial bacterial cellulose was purchased from a local market that used a DOST (Department of Science and Technology)-provided *nata* starter.

### 2.2. Extraction of silk fibroin

A schematic diagram of the experimental procedure is presented in Figure 1. Aqueous SF solutions were prepared at the Philippine Genome Center's (PGC) Protein, Proteomics, and Metabolomics Facility (PPMF). A degumming step was employed by boiling a predetermined weight of SF in 0.02 M sodium carbonate buffer at 70 °C for 45 min. After boiling, the fibers were washed with ultra-pure water and boiled in a carbonate buffer for another 45 min. This cycle was repeated until the wash had cleared. The resulting fibers were dried at 60 °C for 2 days. Post-drying, the silk was dissolved in Ajisawa's solvent composed of a 1:2:8 ratio of $CaCl_2$, EtOH, and (ultra-pure) $H_2O$, respectively. Aqueous silk fibroin was dialyzed against distilled water (MWCO 3500) for 3 days with frequent changing of dialysate every 12 h at 4 °C. Once salt removal was performed, the resulting solution was centrifuged at 4000 rpm, and the supernatant was stored at 4 °C until further use. Batches of extractions resulted in silk fibroin concentrations averaging at approximately 1.0% to 2.0% w/v.

### 2.3. Synthesis of BC-SF composite

A commercial bacterial cellulose pellicle was cut into smaller cubes with consistent dimensions. These dimensions were chosen to meet the minimum requirements for certain mechanical analyses.

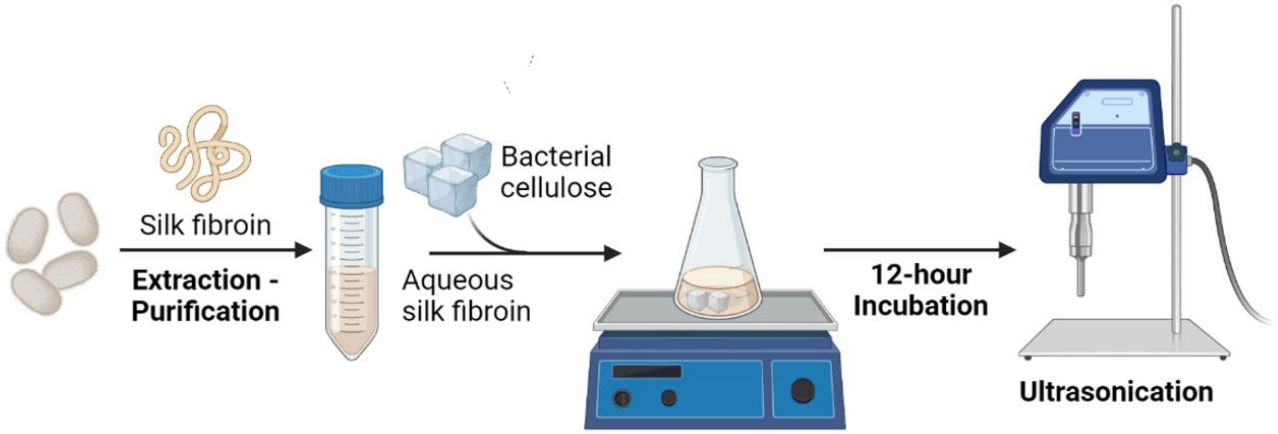


**Scheme 1** Diagram of preparation methods for developing BC-SF composites.

 DOI: 10.15826/chimtech.2024.11.1.07

Cellulose purchased from a local supplier was rinsed using a 0.1 M NaOH solution, followed by several washes with ultrapure water. The pre-cut bacterial cellulose (BC) was measured and divided into dimensions of several ranges. An average dimension size of 9 to 12 mm (length), 2 mm (width), and 2 mm (height) was used. A solution of extracted fibroin (average 1.0% w/v) was used to incubate the BC hydrogels for 48 h at 4 °C. After incubation, a batch of SF-soaked BC hydrogels was sonicated (Witeg WUC-D22H) at a constant amplitude (40%) for varying periods ($t$ = 0, 1, 5, 15, 30, and 60 min). At predetermined time intervals, one BC-SF composite was removed from the sonicated solution. The composite was rinsed three times with ultrapure water and allowed to dry in air at 4 °C until further analysis. A control bacterial cellulose hydrogel (BC) was stored with a synthesized BC-SF composite (BC-SF). The simultaneous batch of sonicated SF (SF (son)) and native silk fibroin (SF (cont)) was also stored at 4 °C.

### 2.4. Characterization

#### 2.4.1. Regenerated silk fibroin (SF)

Fluorescent thioflavin T (ThT) assay was used to determine the β-sheet content over time. A stock solution of 40 mM ThT was prepared. Solutions at 1:6 ratios (Thioflavin T dye to sample) were prepared and measured at excitation and emission wavelengths of 440(10) nm and 480(20) nm respectively. Measurements were taken at 30 s cycles over 9 cycles using a COSTAR 96 black well plate. Secondary protein structure distribution was further verified by circular dichroism spectropolarimetry (Jasco J-1500) equipped with Peltier Thermostat Cellholder (PTC). CD analysis was done in photometric mode simultaneous with HT measurement. The measurement was conducted over a 250–190 nm range with a bandwidth of 10.00 nm and data pitch at 0.1 nm. Analysis was regulated at 27 °C using 1 mm quartz cuvettes and ultrapure water as a blank.

#### 2.4.2. Silk fibroin-bacterial cellulose (SF-BC) composite

Fourier Transform infrared spectroscopy (Thermo Scientific Nicolet 6700 ATR FT-IR Spectrometer, OMNIC Macros software version 3.0) was used to analyze the chemical properties and to assess the changes in the chemical composition of the synthesized composite. Cold field-emission scanning electron microscopy (Ultra-high Resolution CFE-SEM Hitachi SU8600) was done to view the freeze-dried composites at varying magnifications from x250 up to x5,000. A scale bar of 200 um up to 5 um was applied. Simultaneous thermal analyzers, including a differential scanning calorimeter (TA Instruments DSC 25) and a thermogravimetric analyzer (TA Instruments TGA) were used to measure the weight change and differential heat flow of the sample composites.

### 2.5. Statistical analysis

Statistical analysis method was used in order to analyze the results obtained. One-way analysis of variance (one-way ANOVA) test with $p < 0.005$ was used to determine whether the composites (BC, BC+SF(son), and SF (cont)) had significant differences in exposed functional groups dictated by protein conformation.

## 3. Results and Discussion

### 3.1. Thioflavin T Assay and CD spectropolarimetry of β-sheet structures

The sol-gel transitive behavior of regenerated silk fibroin has been an area of interest, as it demonstrates a promising model for the build-up of a gel network and the consequential physicochemical properties. This transition in secondary structure conformations was found to be caused by the ultrasonic energy cleaving longer silk fibroin chains [22]. These chains result in the reorganization of the peptides from alpha-helices to random coiling (silk I) and, finally, to beta-sheet structures (silk II). Data from the Thioflavin T assay supported the increase in beta-sheet conformational structures, as observed in the increase in the fluorescent signals at longer ultrasonication treatment times, as shown in Figure 1.

This was further supported by secondary structure analysis of the CD spectra, showing a peak in beta-sheet structures for SF samples ultrasonicated at 30 seconds. In contrast to the general trend, a decrease in both beta-sheet content via ThT and CD spec was observed for SF ultrasonicated at 60 seconds (Figure 2). This decrease may be caused by the conversion of the protein to a tertiary form, as blocks of β-sheet structures stack to ‘crystallize’ onto a higher level of organization.

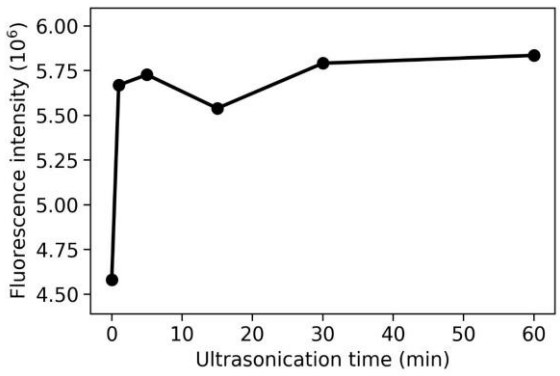


**Figure 1** Thioflavin T assay β-sheet monitoring of ultrasonicated silk fibroin (SF).

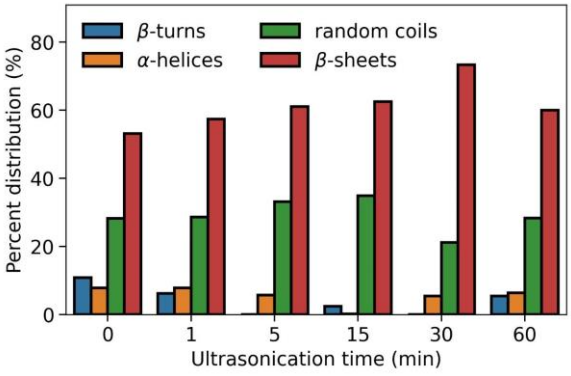


**Figure 2** Secondary structure distribution of ultrasonicated silk fibroin (SF).

 DOI: 10.15826/chimtech.2024.11.1.07

Crystallization of SF into a tertiary structure was hypothesized to be due to the batch molecular weight and working concentration (3±2.5% w/v) [23]. A lower concentration stock of silk fibroin yielded a more stable protein polymer. Ultrasonication of silk fibroin prepared in lower concentrations also allowed for a more representative model of the protein's folding behavior.

### 3.2. Infrared spectroscopy

The synthesized BC-SF composite ultrasonicated for 60 seconds was compared against the control BC as shown in Figure 3. Infrared spectra revealed characteristic peaks exhibited in (unsonicated) silk fibroin still present in (sonicated) silk fibroin, indicative of dominant silk I-type structures in the protein (Figure 4). The peaks attributed to BC included absorption peaks at 3455 $cm^{-1}$ (O–H stretching), 1564 $cm^{-1}$ (C–H), 1070 $cm^{-1}$ (C–O stretching), and 578 $cm^{-1}$ (C–H rocking vibration). These peaks were confirmed in other published work by Tamrin and Atykyan [24, 25]. Similarly, the signature amide I band (1625–1763 $cm^{-1}$) was distinctly observed in control silk fibroin. Strong broad peaks with slight increases in wavenumber were found for both SF and BC-SF at 3267–3388 $cm^{-1}$ (N–H and O–H), 1239–1250 $cm^{-1}$ (C–O–C vibrations), and 1059–1062 $cm^{-1}$ (H-bonding) [26]. This wavenumber increase and broadening of peaks implied the formation of H-bonding between BC and SF. More so, unique peaks were observed for BC-SF at 1519–1548 $cm^{-1}$ (amide II conversion) and 1337 $cm^{-1}$ (amide III conversion) implying the dominant conversion of amide I into amide II and amide III structures [27].

### 3.3. Cold field emission scanning electron microscopy

Images of the surface morphology of silk fibroin, crystalline cellulose, and the BC-SF composite were compared (Figure 5). Crystallized silk fibroin was observed to align with the unidirectional orientation of the BC fibers. Structures less than 1 um can be observed to 'coat' the fibers giving a webbed and matted appearance. The unique silk structures on the surface of BC were found to be consistent with the work of Chen et al. (2017) where the protein was hypothesized to grow on existing 'seeds of crystal' [20]. This is presumed to occur during the ultrasonication process, where proteins would more likely 'fold' when in spatial proximity with other hydrophobic blocks.

**Table 1** Infrared spectroscopy peaks ($cm^{-1}$) for SF, BC, and BC-SF.

| Silk Fibroin | Bacterial cellulose | BC-SF |
|---|---|---|
| 715 | 841 [a] | 955 [a] |
| 1059 [a] | 1021 [a], 1070 [a,b], | 1062 [a,b], 1167 [a], |
| 1239 | 1115 [a,b], 1173 [a,b] | 1250, 1337 |
| 1519 | 1453 [a], 1564, | 1411, 1450 [a], |
| 1625, 1763 [a] | 1684 | 1548, 1651 |
| 3067, 3267, 3658 | 3062, 3455 | 3388 |

[a] Peak found in $p<0.05$ region.
[b] Consistent with reference literature.

The initial nucleation of silk crystals was reported to be determined by characteristic polymer-protein interactions and environmental factors. This study revealed that silk fibroin and bacterial cellulose interactions may have induced some silk I to silk II conversion. However, it was more likely brought about by the ultrasonication treatment.

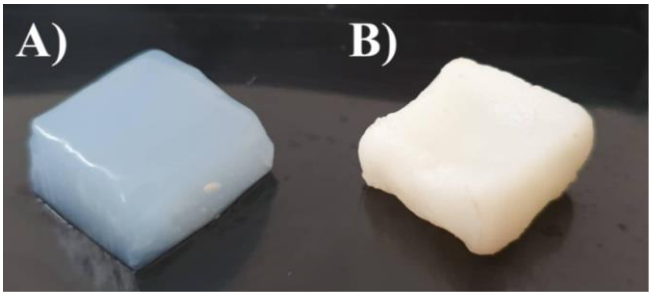


**Figure 3** Control BC hydrogel (a) and ultrasonicated BC hydrogel + silk fibroin (BC-SF) (b).

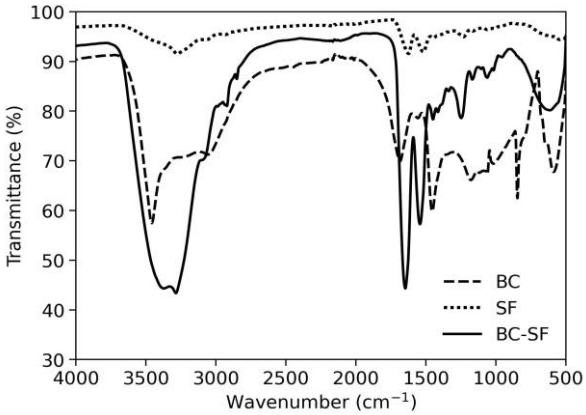


**Figure 4** Overlay FT-IR spectra of BC, SF, and BC-SF composites.

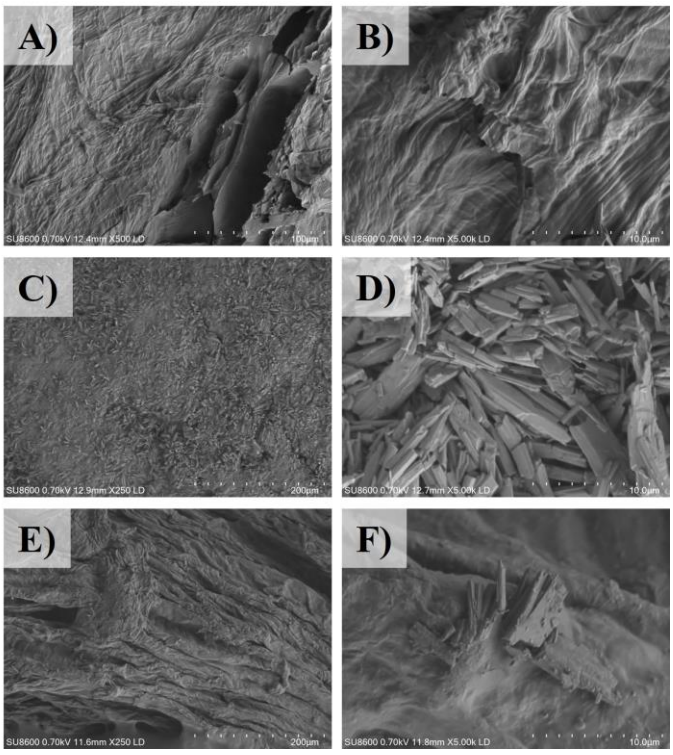


**Figure 5** Scanning electron microscopic images of the surface of lyophilized regenerated silk fibroin (a, b), crystalline bacterial cellulose (c, d), and synthesized BC-SF composites (e, f).

 DOI: 10.15826/chimtech.2024.11.1.07

### 3.4. Differential scanning calorimetry and thermogravimetric analysis

The data from the thermogravimetric analysis also demonstrated that the developed composite was more thermodynamically stable, given the more gradual loss of biomass over the specified temperature range (Figures 6, 7). Unlike its untreated counterpart, control microbial cellulose was observed to lose both water and mass faster compared to BC-SF, suggesting the more thermodynamically stable bio composite compared to the control (BC). It can be inferred that the weight loss (%) observed from 40 °C to 300 °C can be attributed to water losses, as it is present in all curves. Furthermore, fibroin decomposition can be observed in the 300 °C to 500 °C range, with the decomposition of cellulose fibers starting at 500 °C. The composite is observed to resist heat degradation at around 530 °C prior to its ultimate disintegration. This is in agreement with the findings of the work of Barud et al. [25].

DSC curves are observed to share a baseline at around 150 °C indicating a glass transition event (due to loss of water) and endothermic peaks at 130.18 °C, 141.92 °C, and 167.81 °C for SF, BC, and BC-SF respectively. The heat-flow temperature curves also demonstrate varying stages of 'melting'. The first melting peak can be attributed to the decomposition of amino acids exhibited by SF.

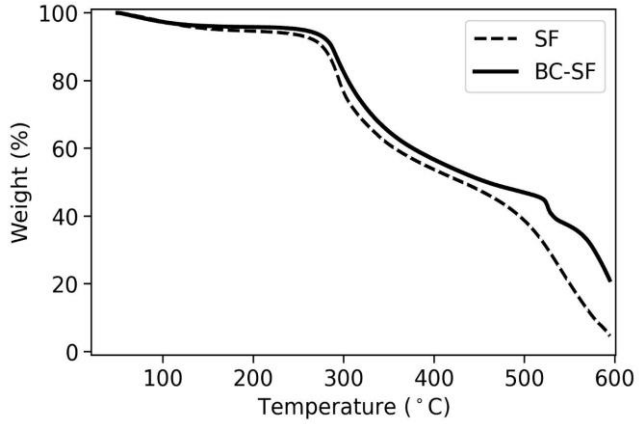


**Figure 6** TGA curves of untreated pure SF, BC, and treated BC-SF.

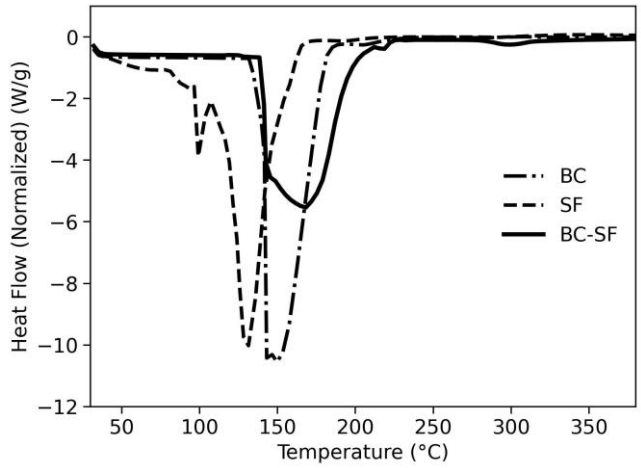


**Figure 7** DSC profiles of untreated pure SF, BC, and treated BC-SF.

The sharp endothermic peak of BC is consistent with its pure polymeric nature. This is in contrast to the flatter BC-SF peak which is only partially crystalline due to the embedded silk fibroin crystals. The broader peak is an expected consequence of ultrasonication of silk fibroin, as it would lead to a wider size distribution of crystallites.

## 4. Limitations

This study has limited its analyses to physicochemical and mechanical properties of the composite.

## 5. Conclusions

Commercial bacterial cellulose was used as a 'scaffold' for regenerated silk fibroin to be absorbed between the cellulose fibers. The absorbed silk fibroin was then 'locked in' via ultrasonication, allowing the silk fibroin to convert some of its previously dominant silk I into silk II structures. This characteristic is helpful in the stabilization of silk protein when used for unique composite applications that require slowed amyloid formation. Future research should explore cytotoxicity and cell culturing tests to determine the material's viability for tissue engineering applications. Furthermore, the promising thermal analysis data suggests that tensile and compressive strength tests should be done to check for the overall yield strength of the composite.

## • Supplementary materials

No supplementary materials are available.

## • Funding

The authors want to acknowledge funding from the Research & Grants Management Office (RGMO) of De La Salle University – Manila (Project number: 16 FU1TAY20-1TAY22).

## • Acknowledgments

The authors would like to acknowledge the contributions of Mr. John Paulin, Mr. Bernard, Ms. Patricia Palomillo, and Mr. Robert Jervine Ortega. We would also like to acknowledge Sigmatech PH for allowing us to run our samples during our visit to their facility.

## • Author contributions

Conceptualization: M.S.C., F.F.Jr.
Data curation: M.S.C., M.C.T.
Formal Analysis: M.S.C., N.A.B.
Funding acquisition: F.F.Jr., M.C.T.
Investigation: M.S.C.
Methodology: M.S.C.
Project administration: F.F.Jr., M.C.T.
Resources: M.S.C., F.F.Jr.

 DOI: 10.15826/chimtech.2024.11.1.07

Software: M.S.C.
Supervision: M.C.T., N.A.B.
Validation: M.C.T., N.A.B.
Visualization: F.F.Jr.
Writing – original draft: M.S.C., F.F.Jr.
Writing – review & editing: M.S.C., F.F.Jr.

## • Conflict of interest

The authors declare no conflict of interest.

## • Additional information

Author IDs:

Mary Stephanie Carranza, Scopus ID 57203552245;
Neil Andrew D. Bascos, Scopus ID 6504041963;
Maria Carmen Tan, Scopus ID 56079458200;
Francisco Franco Jr., Scopus ID 57217531264.

Website:

University of the Philippines System – Philippine Genome Center, https://pgc.up.edu.ph/;
De La Salle University, https://www.dlsu.edu.ph/.

## References

1. Angelova N, Hunkeler D. Rationalizing the design of polymeric biomaterials. Trends Biotechnol. 1999;17:409–421. doi:10.1016/s0167-7799(99)01356-6
2. Liu J, Ge X, Liu L, Xu W, Shao R. Challenges and opportunities of silk protein hydrogels in biomedical applications. Mater Adv. 2022;3:2291–2308. doi:10.1039/D1MA00960E
3. Koh LD, Cheng Y, Teng CP, Khin YW, Loh XJ, et al. Structures, mechanical properties and applications of silk fibroin materials. Prog Polym Sci. 2015;46:86–110. doi:10.1016/j.progpolymsci.2015.02.001
4. Wang C, Xia K, Zhang Y, Kaplan DL. Silk-based advanced materials for soft electronics. Acc Chem Res. 2019;52:2916–2927. doi:10.1021/acs.accounts.9b00333
5. Huang W, Ling S, Li C, Omenetto FG, Kaplan DL. Silkworm silk-based materials and devices generated using bio-nanotechnology. Chem Soc Rev. 2018;47:6486–6504. doi:10.1039/c8cs00187a
6. Hardy JG, Scheibel TR. Composite materials based on silk proteins. Prog Polym Sci. 2010;35:1093–1115. doi:10.1016/j.progpolymsci.2010.04.005
7. Matsumoto A, Chen J, Collette AL, Kim U-J, Altman GH. Mechanisms of silk fibroin sol–gel transitions. J Phys Chem B. 2006;110:21630–21638. doi:10.1021/jp056350v
8. Kim UJ, Park J, Li C, Jin HJ, Valluzzi R, et al. Structure and properties of silk hydrogels. Biomacromolec. 2004;5:786–792. doi:10.1021/bm0345460
9. Choi Y, Cho SY, Heo S, Jin HJ. Enhanced mechanical properties of silk fibroin-based composite plates for fractured bone healing. Fibers Polym. 2013;14:266–270. doi:10.1007/s12221-013-0266-5
10. Gregory DA, Tripathi L, Fricker ATR, Asare E, Orlando I, et al. Bacterial cellulose: a smart biomaterial with diverse applications. Mater Sci Eng R Rep. 2021;145:100623. doi:10.1016/j.mser.2021.100623
11. Phisalaphong M, Chiaoprakobkij N. Applications and products-nata de coco in bacterial nano cellulose. CRC Press. 2016;143. doi:10.1201/b12936-8
12. Gallegos AMA, Herrera CS, Parra R, Keshavarz T, Iqbal HMN. Bacterial cellulose: a sustainable source to develop value-added products – a review. BioResources. 2016;11:5641–5655.
13. Jung HI, Jeong JH, Lee OM, Park GT, Kim KK, et al. Influence of glycerol on production and structural–physical properties of cellulose from Acetobacter sp. V6 cultured in shake flasks. Bioresour Technol. 2010;101:3602–3608. doi:10.1016/j.biortech.2009.12.111
14. Castro C, Zuluaga R, Putaux JL, Caro G, Mondragon I et al. Structural characterization of bacterial cellulose produced by Gluconacetobacter swingsii sp. from Colombian agroindustrial wastes. Carbohydr Polym. 2011;84:96–102. doi:10.1016/j.carbpol.2010.10.072
15. Czaja W, Romanovicz D, Brown RM. Structural investigations of microbial cellulose produced in stationary and agitated culture. Cellulose. 2004;11:403–411. doi:10.1023/B:CELL.0000046412.11983.61
16. Gea S, Reynolds CT, Roohpour N, Wirjosentono B, Soykeabkaew N et al. Investigation into the structural, morphological, mechanical and thermal behaviour of bacterial cellulose after a two-step purification process. Bioresour Technol. 2011;102:9105–9110. doi:10.1016/j.biortech.2011.04.077
17. Portela R, Leal CR, Almeida PL, Sobral RG. Bacterial cellulose: a versatile biopolymer for wound dressing applications. Microb Biotechnol. 2019;12:586–610. doi:10.1111/1751-7915.13392
18. Lee JM. The fixation effect of a silk fibroin–bacterial cellulose composite plate in segmental defects of the zygomatic arch: an experimental study. JAMA Otolaryngol. Neck Surg. 2013;139:629–635. doi:10.1001/jamaoto.2013.3044
19. Wang X, Kluge JA, Leisk GG, Kaplan DL. Sonication-induced gelation of silk fibroin for cell encapsulation. Biomater. 2008;29:1054–1064. doi:10.1016/j.biomaterials.2007.11.003
20. Chen J, Zhuang A, Shao H, Hu X, Zhang Y. Robust silk fibroin/bacterial cellulose nanoribbon composite scaffolds with radial lamellae and intercalation structure for bone regeneration. J Mater Chem B. 2017;5:3640–3650. doi:10.1039/C7TB00485K
21. Wang K, Ma Q, Zhang YM, Han GT, Qu CX, Wang SD. Preparation of bacterial cellulose/silk fibroin double-network hydrogel with high mechanical strength and biocompatibility for artificial cartilage. Cellulose. 2020;27:18745–1852. doi:10.1007/s10570-019-02869-0
22. Yuan T, Li Z, Zhang Y, Shen K, Zhang X, Xie R, Liu F, Fan W. Injectable ultrasonication-induced silk fibroin hydrogel for cartilage repair and regeneration. Tissue Eng Part A. 2021;27(17–18):1213–1224. doi:10.1089/ten.TEA.2020.0323
23. Qi Y, Wang H, Wei K, Yang Y, Zheng RY, Kim IS, Zhang KQ. A review of structure construction of silk fibroin biomaterials from single structures to multi-level structures. Int J Mol Sci. 2017;18(3):237. doi:10.3390/ijms18030237
24. Atykyan NA, Revin V, Shutova VV. Raman and FTIR spectroscopy investigation of cellulose structural differences from bacteria *Gluconacetobacter sucrofermentans* during the different regimes of cultivation on a molasses media. AMB Expr. 2020;10:84. doi:10.1186/s13568-020-01020-8
25. Barud HGO, Barud HDS, Cavicchioli M, Amaral TSD, Junior OBDO, Santos DM, Petersen ALDOA, Celes F, Borges VM, Oliveira CIDO, Oliveira PFD, Furtado RA, Tavares DC, Ribeiro SJL. Preparation and characterization of a bacterial cellulose/silk fibroin sponge scaffold for tissue regeneration. Carb Poly. 2015;128:41–51. doi:10.1016/j.carbpol.2015.04.007
26. Hu Y, Zhang Q, You R, Wang L, Li M. The relationship between secondary structure and biodegradation behavior of silk fibroin scaffolds. Adv Mat Sci Eng. 2012:185905. doi:10.1155/2012/185905
27. Carissimi G, Baronio CM, Montalban MG, Villora G, Barth A. On the secondary structure of silk fibroin nanoparticles obtained using ionic liquids: an infrared spectroscopy study. Polymers. 2020;12(6):1294. doi:10.3390/polym12061294

 DOI: 10.15826/chimtech.2024.11.1.07